2016

The action of discoidin domain receptor 2 in basal tumor cells and stromal cancer-associated fibroblasts Is critical for breast cancer metastasis

Callie A.S. Corsa
Washington University School of Medicine in St. Louis

Audrey Brenot
Washington University School of Medicine in St. Louis

Whitney R. Grither
Washington University School of Medicine in St. Louis

Samantha Van Hove Washington University School of Medicine in St. Louis

Andrew J. Loza
Washington University School of Medicine in St. Louis

See next page for additional authors

Authors
Callie A.S. Corsa, Audrey Brenot, Whitney R. Grither, Samantha Van Hove Washington University School of Medicine in St. Louis, Andrew J. Loza, Kun Zhang, Suzanne M. Ponik, Yuming Liu, David G. DeNardo, Kevin W. Eliceiri, Patricia J. Keely, and Gregory D. Longmore

Article

Cell Reports

The Action of Discoidin Domain Receptor 2 in Basal Tumor Cells and Stromal Cancer-Associated Fibroblasts Is Critical for Breast Cancer Metastasis

Graphical Abstract

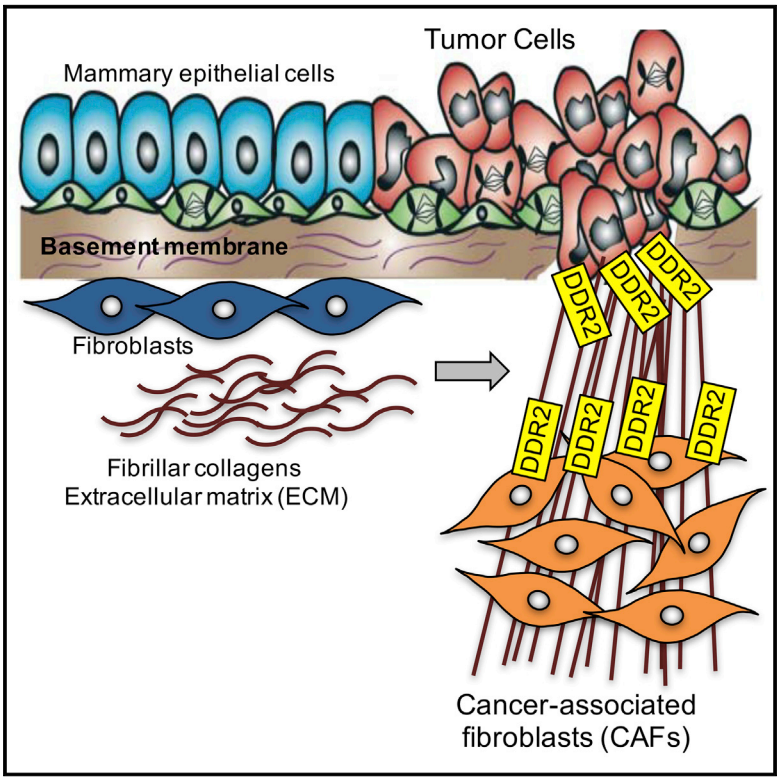

Highlights

- DDR2 activity in both tumor and stromal cells is critical for breast cancer metastasis
- DDR2 regulates collective invasion/migration of basal K14+ breast tumor cells
- In CAFs, DDR2 regulates tumor ECM production and collagen fiber remodeling
- In CAFs, DDR2 enhances tumor collective invasion/migration

Authors

Callie A.S. Corsa, Audrey Brenot, Whitney R. Grither, ..., Kevin W. Eliceiri, Patricia J. Keely, Gregory D. Longmore

Correspondence

glongmore@wustl.edu

In Brief

Using an in vivo genetic approach, Corsa et al. identify the actions of DDR2, a distinctive receptor tyrosine kinase activated by fibrillar collagens, in breast cancer metastasis. DDR2 functions in both tumor and stromal cells of primary tumors, affecting metastasis but not tumor growth.

Corsa et al., 2016, Cell Reports *15*, 2510–2523
June 14, 2016
http://dx.doi.org/10.1016/j.celrep.2016.05.033

CellPress

OPEN ACCESS
CellPress

Cell Reports
Article

The Action of Discoidin Domain Receptor 2 in Basal Tumor Cells and Stromal Cancer-Associated Fibroblasts Is Critical for Breast Cancer Metastasis

Callie A.S. Corsa,[1,2,3] Audrey Brenot,[1,3] Whitney R. Grither,[1,3,4] Samantha Van Hove,[1,2,3] Andrew J. Loza,[1,3,5] Kun Zhang,[1,3] Suzanne M. Ponik,[6] Yuming Liu,[7] David G. DeNardo,[1,3] Kevin W. Eliceiri,[7] Patricia J. Keely,[6,7] and Gregory D. Longmore[1,2,3,*]

[1]ICCE Institute, Washington University, St. Louis, MO 63110, USA
[2]Department of Cell Biology and Physiology
[3]Department of Medicine
[4]Department of Biochemistry
[5]Department of Computational and Molecular Biophysics
Washington University, St. Louis, MO 63110, USA
[6]Department of Cell and Regenerative Biology, University of Wisconsin School of Medicine and Public Health, Madison, WI 53706, USA
[7]Laboratory for Optical and Computational Imaging, University of Wisconsin School of Medicine and Public Health, Madison, WI 53706, USA
*Correspondence: glongmore@wustl.edu
http://dx.doi.org/10.1016/j.celrep.2016.05.033

SUMMARY

High levels of collagen deposition in human and mouse breast tumors are associated with poor outcome due to increased local invasion and distant metastases. Using a genetic approach, we show that, in mice, the action of the fibrillar collagen receptor discoidin domain receptor 2 (DDR2) in both tumor and tumor-stromal cells is critical for breast cancer metastasis yet does not affect primary tumor growth. In tumor cells, DDR2 in basal epithelial cells regulates the collective invasion of tumor organoids. In stromal cancer-associated fibroblasts (CAFs), DDR2 is critical for extracellular matrix production and the organization of collagen fibers. The action of DDR2 in CAFs also enhances tumor cell collective invasion through a pathway distinct from the tumor-cell-intrinsic function of DDR2. This work identifies DDR2 as a potential therapeutic target that controls breast cancer metastases through its action in both tumor cells and tumor-stromal cells at the primary tumor site.

INTRODUCTION

Breast cancer is the second leading cause of cancer-related deaths in women, and more than 90% of mortality is due to metastatic disease. The majority of breast cancers originate in the epithelial cells lining the mammary ducts as a result of hereditary or acquired genetic mutations that largely affect tumor cell growth and survival (Vargo-Gogola and Rosen, 2007). However, tumor development and progression is also accompanied by changes in the surrounding cellular, chemical, and physical environment, and it is now appreciated that these changes in tumor environment contribute to tumor development, progression, and metastasis (Vargo-Gogola and Rosen, 2007; Schedin and Keely, 2011). Although there are many biologic processes contributing to tumor metastasis, the capacity of tumor cells to de-adhere from one another and other epithelial cells and then invade through the basement membrane and migrate through the interstitial space to access lymphatic and vascular channels are clearly important first steps. Tumor cell invasion and migration are regulated by reciprocal communicating pathways between tumor cell and tumor-stromal components.

Women with high mammographic density, which is, in part, due to increased collagen deposition in the breast, have increased risk of developing breast cancer, and when they do, their cancers tend to be more invasive and exhibit poorer prognosis (Boyd et al., 2002). Moreover, in many breast tumors, there is increased deposition of collagen fibers and, when present, this is associated with a worse clinical outcome (Schedin and Keely, 2011). In addition to the prognostic implications of increased tumor collagen, the presence of thick, straight, and long fibers and the alignment of collagen fibers relative to the tumor-stromal boundary (collectively termed the tumor-associated collagen signature, or TACS) are also correlated with invasive disease and poor prognosis (Provenzano et al., 2006, 2008). Despite these clinical associations or correlations, the molecular and cellular mechanisms responsible for increased collagen fiber deposition and collagen fiber remodeling in tumors remain undefined.

Recently, the fibrillar collagen receptor discoidin domain receptor 2 (DDR2) was found to influence breast tumor cell invasion in 2D and 3D culture models as well as breast tumor metastasis in syngeneic and xenogenic orthotopic transplant models (Zhang et al., 2013; Ren et al., 2014). Normal human breast epithelium does not express DDR2, but 50%–70% of invasive ductal carcinomas express DDR2 (Zhang et al., 2013; Toy et al., 2015). DDR2 expression has also been detected in stromal

cells around the tumor (Zhang et al., 2013; Toy et al., 2015). The cellular action of DDR2 has been implicated in collagen synthesis and extracellular matrix (ECM) remodeling (Ferri et al., 2004; Sivakumar and Agarwal, 2010), endothelial cell (EC) functions (Zhang et al., 2014), dendritic cell activation (Lee et al., 2007), and neutrophil migration (Afonso et al., 2013). Targeted ubiquitous deletion of the Ddr2 gene or spontaneous mutations in the Ddr2 gene in mice (*slie* mouse) result in dwarfism due to reduced chondrocyte proliferation during early bone development and impaired wound healing due to defective cell migration (Labrador et al., 2001; Kano et al., 2008). Ddr2-null mice are also infertile due to defects in spermatogenesis and ovulation (Kano et al., 2008, 2010; Matsumura et al., 2009).

To understand the cellular basis for DDR2's action in the regulation of breast cancer metastasis, we used a genetic approach in mouse models of breast cancer metastasis. We generated a number of Ddr2 mouse alleles, including a conditional allele and a cell-marker-tracking allele. We found that the action of DDR2 in both primary tumor cells and primary tumor stromal cancer-associated fibroblasts (CAFs) is critical for breast cancer metastasis in the mouse mammary tumor virus-polyoma middle T antigen (MMTV-PyMT) mouse model, without affecting primary tumor growth.

RESULTS

Generation and Characterization of Modified DDR2 Alleles in Mice

To determine the cellular basis of DDR2 action in breast cancer metastasis in vivo, we generated multiple Ddr2 alleles using targeted embryonic stem cells obtained from the European Conditional Mouse Mutagenesis Program (EUCOMM). The mouse Ddr2 gene is located on chromosome 1, contains 19 exons, and encodes a single transcript that produces just one protein isoform. The EUCOMM-targeted Ddr2 allele contains a lacZ reporter gene and a neomycin gene, each with polyadenylation sequences that terminates transcription. These cassettes are inserted between exons 7 and 9 of the Ddr2 gene, which encode for a portion of the extracellular DS-like domain. Two FRT sites bracketing the lacZ and neomycin sequences and three loxP sites allow for the generation of either a null allele or a conditional allele when recombined (Figure 1A). The original targeted allele is a Ddr2-null that expresses lacZ under the control of Ddr2 transcriptional regulatory elements ($Ddr2^{null}$). To enhance expression of lacZ, we crossed the original Ddr2 allele to β-actin-Cre mice to excise the neomycin gene and exon 8 ($Ddr2^{lacZ}$; Figures 1A and S1A), thereby generating another Ddr2-null allele.

To generate a conditional allele, we crossed the original Ddr2 allele to FLP^{O} transgenic mice, which resulted in the deletion of the lacZ and neomycin cassette, leaving two loxP sites flanking exon 8 ($Ddr2^{fl}$; Figures 1A and S1B). Subsequent Cre-mediated recombination of the two remaining loxP sites resulted in the deletion of exon 8 and a frameshift mutation that introduced a stop codon in exon 10, which encodes for part of the extracellular domain of DDR2 just outside the transmembrane region ($Ddr2^{-}$).

To generate ubiquitous DDR2-null mice, we crossed the original $Ddr2^{null/+}$ founders. $Ddr2^{null/null}$ mice were 25% smaller than their wild-type (WT) littermates (Figures 1B and 1C) and sterile, as previously reported (Labrador et al., 2001; Kano et al., 2008). $Ddr2^{lacZ/lacZ}$ and $Ddr2^{-/-}$ mice were also dwarves and infertile. Western blot analysis of dermal fibroblasts isolated from $Ddr2^{null/null}$ mice confirmed deletion of the DDR2 protein (Figure 1D). Homozygous conditional $Ddr2^{fl/fl}$ mice did not display any phenotypic abnormalities and bred in normal Mendelian ratios. When these mice were crossed with β-actin-Cre to produce ubiquitous $Ddr2^{-/-}$ mice, PCR analysis revealed successful deletion of the floxed exon 8, indicating that the loxP sites are functional in vivo (Figure 1E). These $Ddr2^{-/-}$ mice were also dwarves and infertile. Western blot analysis of dermal fibroblasts isolated from these mice also revealed deletion of the DDR2 protein (Figure 1F). Mammary gland development was not affected by Ddr2 gene deletion in all three ubiquitous DDR2-null mice (Figures S1C–S1E). Both mammary ductal branching and terminal end bud numbers were unchanged from WT littermates.

Ubiquitous Deletion of DDR2 Reduces Breast Cancer Metastasis to the Lung without Affecting Primary Tumor Growth

MMTV-PyMT transgenic mice develop multifocal primary tumors in the mammary glands beginning as early as 3 weeks of age, and over 90% of these mice go on to develop lung metastases (Guy et al., 1992; Kim and Baek, 2010). Tumors progress through stages similar to human breast cancer: hyperplasia, adenoma, and, finally, invasive adenocarcinoma and metastases (Kim and Baek, 2010). To determine whether DDR2 influenced breast cancer development and metastasis in genetic mouse models, we generated ubiquitous $Ddr2^{null/null}$; MMTV-PyMT mice. There was no difference in latency of primary tumor formation or time (14 weeks) for tumors to reach maximum size (2 cm) between $Ddr2^{+/+}$ and $Ddr2^{null/null}$ mice (Figure 2A). DDR2 deletion did not affect the number of primary tumors or total primary tumor burden per mouse (Figures 2B and S2A). There was no difference in level of Ki-67 staining in primary tumors from $Ddr2^{+/+}$ versus $Ddr2^{-/-}$ mice (Figure S2B). These results indicated that, in vivo, the action of DDR2 did not affect growth of primary tumors in the MMTV-PyMT mouse model of breast cancer.

In stark contrast, there was dramatic reduction in the number of macroscopic and microscopic metastases in the lungs of $Ddr2^{null/null}$ mice (Figures 2C and S2C). Similar results were obtained with three different ubiquitous DDR2-null mice ($Ddr2^{null/null}$, $Ddr2^{lacZ/lacZ}$, and $Ddr2^{-/-}$) (Figure 2C). When present, we did not observe any difference in the average size of individual lung metastases, between WT and DDR2-null mice (Figure S2D). These data indicated that DDR2 played a critical role in the progression of breast cancer to lung metastasis in the MMTV-PyMT mouse model.

Both Tumor and Tumor-Associated Stromal Cells Express DDR2 as Breast Tumors Develop, Progress, and Metastasize

Immunohistochemistry (IHC) analyses of human breast cancers have revealed that DDR2 is expressed in the majority of invasive ductal carcinoma cells yet not in normal breast epithelial tissue (Zhang et al., 2013; Toy et al., 2015). Given that available mouse DDR2 antibodies do not specifically detect DDR2 in mouse

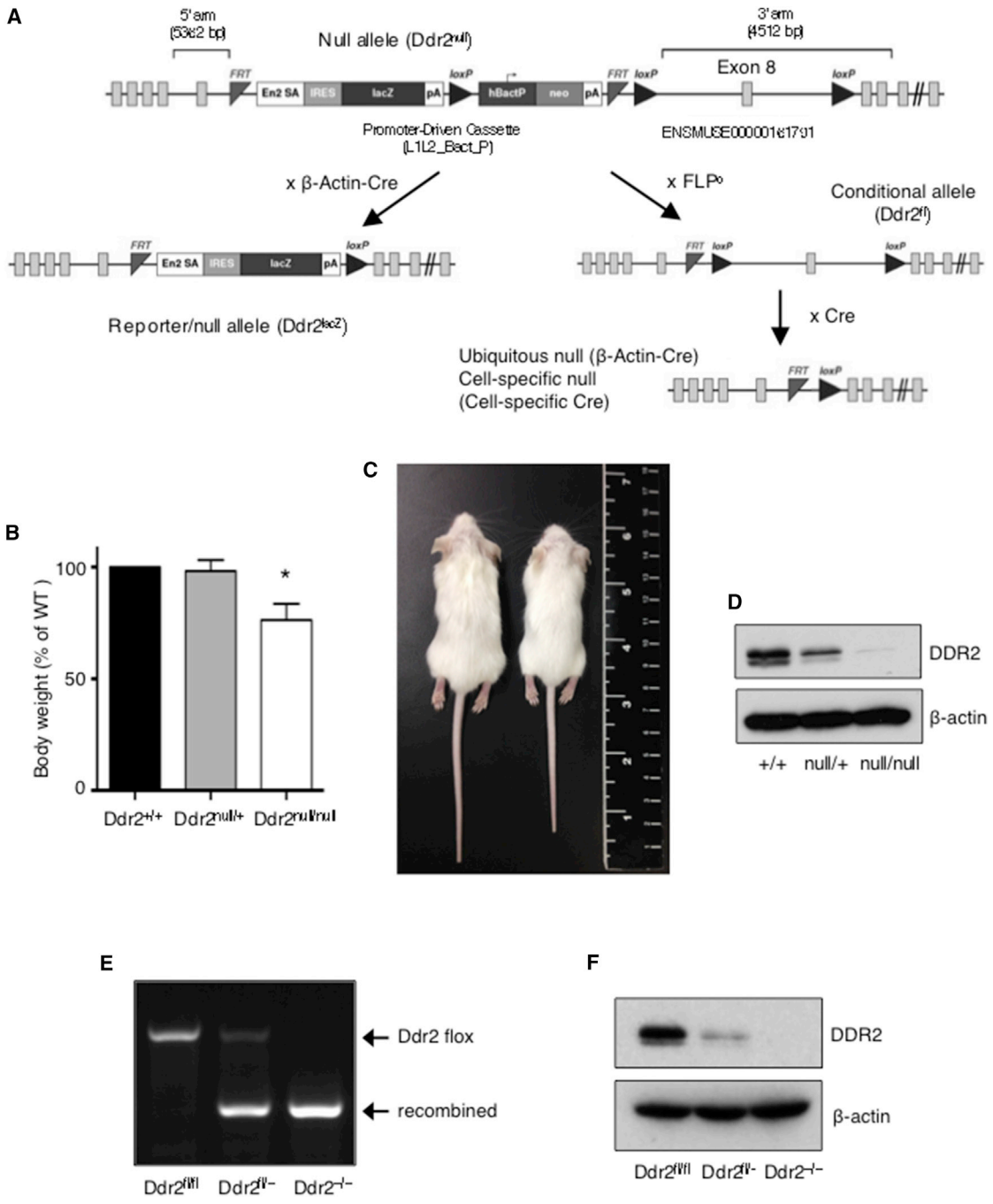

Figure 1. Generation and Characterization of Modified Mouse DDR2 Alleles

(A) Schematic of Ddr2 alleles. $Ddr2^{null}$ mice were crossed with β-actin-Cre mice to generate the $Ddr2^{lacz}$ allele. $Ddr2^{null}$ mice were crossed with FLP^{O} mice to generate the conditional floxed allele ($Ddr2^{fl}$).

(B) Body weights of various mice, calculated as percentage of WT littermate. *$p < 0.001$, ten mice per group. Data are presented as mean ± SD.

(C) Representative images confirming the dwarfism phenotype in $Ddr2^{-/-}$ mice.

(D) Western blot of extracts from dermal fibroblasts isolated from $Ddr2^{+/+}$ and $Ddr2^{null/null}$ mice with indicated antibodies.

(E) PCR detection of floxed and recombined DDR2 alleles in dermal fibroblasts isolated from indicated mice.

(F) Western blot of extracts from dermal fibroblasts isolated from indicated mice, with the indicated antibodies.

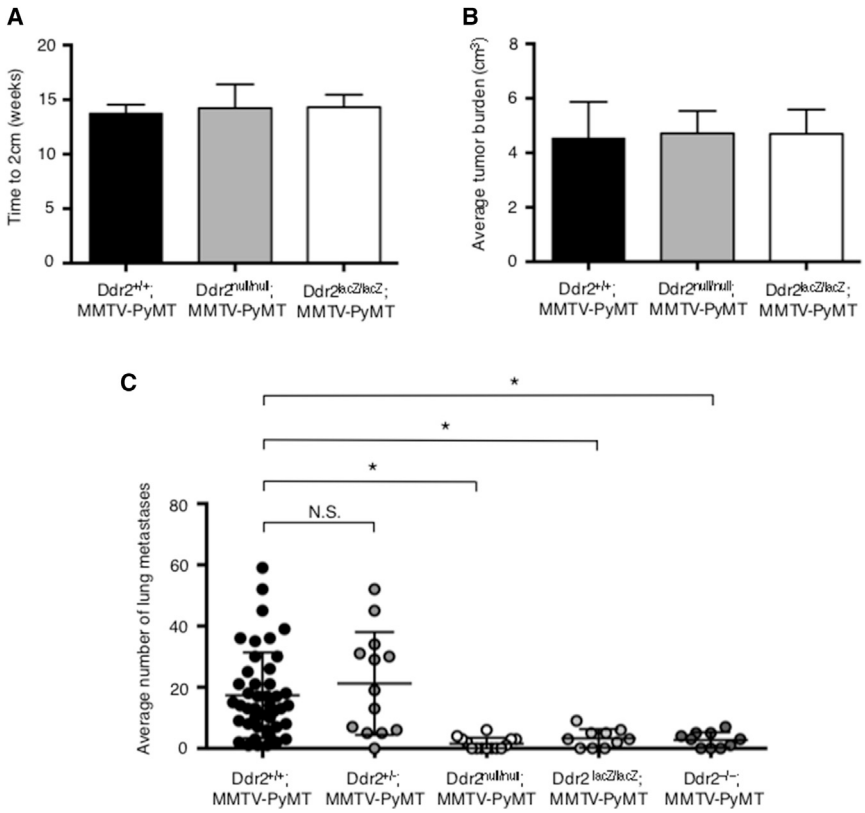

Figure 2. Ubiquitous Deletion of DDR2 Reduces Breast Cancer Lung Metastasis without Affecting Primary Tumor Growth

(A) Primary MMTV-PyMT tumor growth rates in indicated mice, determined by the age at which the largest tumor reached 2 cm in diameter. 10–40 mice per group. Data are presented as mean ± SD.

(B) Total tumor burden of indicated mice, determined by the sum of the volume of all tumors for each mouse when the largest tumor reached 2 cm in diameter. Tumor volumes were calculated by $V = 0.52 \times (W^2) \times L$. 10–40 mice per group. Data are presented as mean ± SD.

(C) Quantification of number of lung metastases in indicated mice calculated by the average number of microscopically visible metastases counted from three H&E-stained sections of lung from each mouse taken 200 μm apart and normalized to the total lung area. *$p < 0.01$; N.S., not significant. 10–40 mice per group. Data are presented as mean ± SD.

tissues by IHC or immunofluorescence (IF), we made use of the $Ddr2^{lacZ}$ allele to track DDR2 expression during MMTV-PyMT breast cancer development. X-gal staining revealed low-level DDR2 expression in stromal cells of normal mammary gland, but no staining was apparent in normal breast epithelial cells (Figure 3A). DDR2 expression (LacZ) was detected in MMTV-PyMT tumor cells of early hyperplastic lesions, adenomas, and adenocarcinomas (Figure 3A). Higher magnification views of early hyperplastic lesions revealed that most DDR2-expressing tumor cells were at the ductal-stromal interface (Figure 3B). In addition, both luminal and basally located epithelial tumor cells, and tumor-associated stromal cells stained positive for X-gal (Figure 3B). DDR2 expression was also present in metastatic lung tumors but not normal lung epithelium (Figures S2E and S2F).

To confirm the identity of DDR2-positive cells in breast tumor, we performed X-gal and IF staining on serial sections, using antibodies specific for basal myoepithelial cells (alpha-smooth muscle actin [α-SMA] and cytokeratin 14 [K14]) and luminal epithelial cells (cytokeratin 8 [K8]). DDR2 was detected in both luminal ($K8^+$) and basal ($K14^+$) epithelial-like tumor cells in hyperplastic lesions (Figure 3C). To co-localize DDR2 expression with specific cell markers in the same tissue slice, we performed dual-color in situ hybridization (ISH) for mRNA. This analysis also revealed that DDR2 was expressed in $K8^+$ and $K14^+$ cells in 13-week MMTV-PyMT breast carcinomas (Figure 3D).

Breast tumor stromal cell expression of DDR2 has been observed in human breast cancer, but the precise identity of these cells has not been determined (Zhang et al., 2013; Toy et al., 2015). Dual-color ISH with fibroblast activation protein (FAP) (to detect CAFs) and DDR2 revealed that DDR2 was expressed in stromal CAFs (Figure 6B). This was confirmed by western blot analysis of isolated primary human breast CAFs (Figure 6A). Dual ISH with the pan-leukocyte marker (CD45) and DDR2 gave ambiguous results, so we sorted for $CD45^+$ cells from 13-week WT breast carcinomas and then performed qPCR for DDR2 and GAPDH controls. DDR2 mRNA was detected in $CD45^+$ tumor-associated stromal cells (Figure S2G).

These analyses in mouse MMTV-PyMT breast tumors at multiple stages of development revealed that, like human breast tumors, DDR2 was not expressed in normal breast epithelial cells, but both luminal and basal epithelial cells expressed DDR2 in tumors. In the tumor stroma, DDR2 was expressed in CAFs and $CD45^+$ pan-leukocyte cells. Lung metastases also expressed DDR2.

Action of DDR2 in Basal, but Not Luminal, Breast Epithelial Cells Is Critical for Lung Metastasis

Next, we set out to determine the contribution of the action of DDR2 in luminal and basal-like tumor epithelial cells to primary breast tumor growth and metastasis in a mouse genetic model. To do so, the Ddr2 gene was selectively deleted in mammary luminal epithelial cells using MMTV-Cre or in basal and luminal epithelial cells using K14-Cre (Dassule et al., 2000; Wagner et al., 2001). Although K14 expression is restricted to basal cells soon after birth, during early stages of mammary gland development, K14 is expressed in both basal and luminal epithelial cells (Van Keymeulen et al., 2011); therefore, K14-Cre allows for deletion of Ddr2 in both breast epithelial cell types.

$Ddr2^{fl/fl}$; MMTV-Cre and $Ddr2^{fl/fl}$; K14-Cre mice were crossed to MMTV-PyMT mice. In agreement with results from ubiquitous Ddr2-null mice, we observed no differences in primary tumor

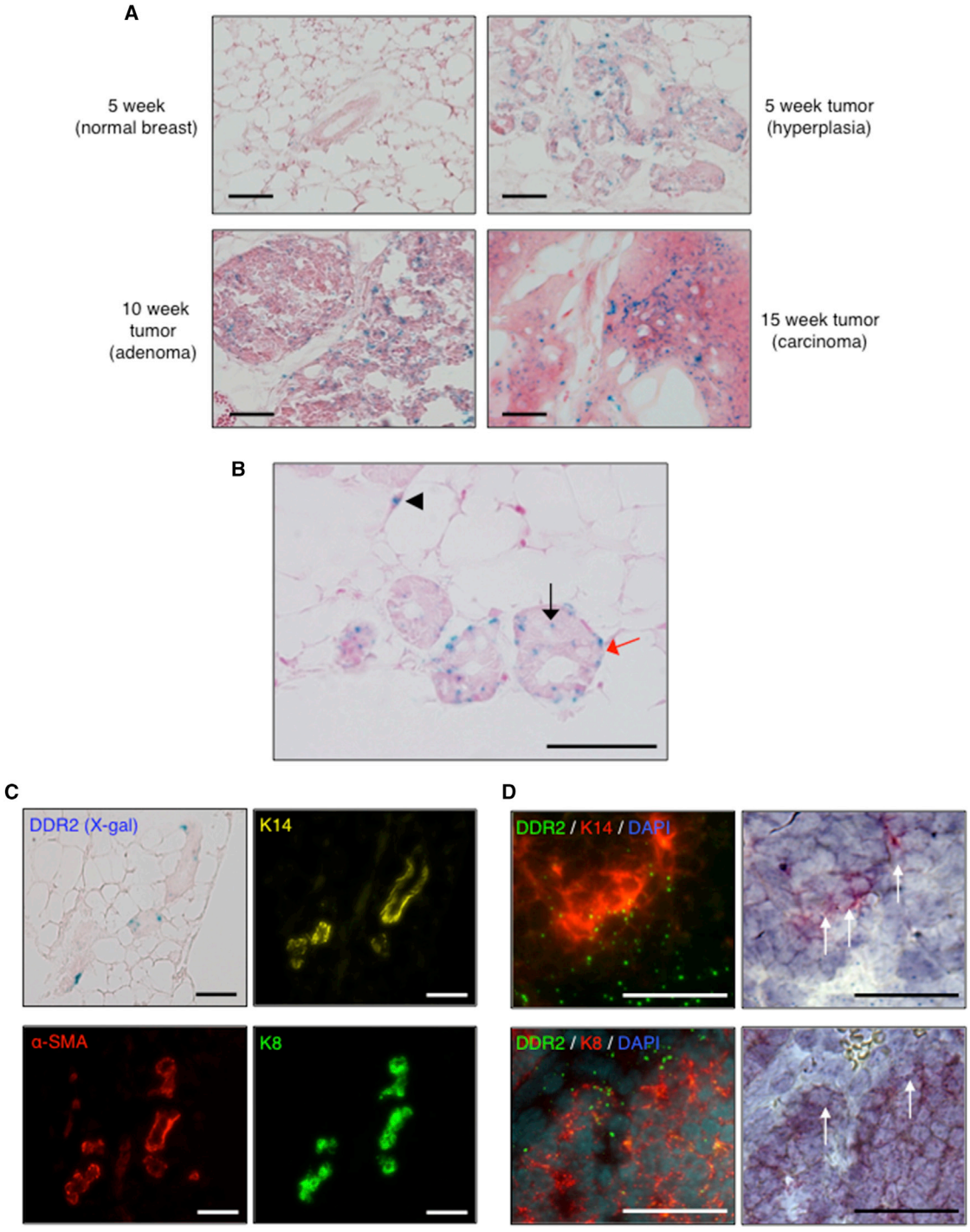

Figure 3. DDR2 Expression in Mouse MMTV-PyMT Breast Tumor Development and Progression

(A) X-gal staining of mammary gland/tumor sections from Ddr2$^{lacZ/+}$; MMTV-PyMT mice at multiple times during tumor development. Scale bars, 50 μm.

(B) X-gal staining on hyperplastic mammary glands from 5-week-old Ddr2$^{lacZ/+}$; MMTV-PyMT mice. Scale bars, 50 μm. Arrowhead indicates stromal cell, black arrow indicates luminal epithelial cell, and red arrow indicates basal myoepithelial cell.

(C) X-gal staining and immunofluorescence for K14 (yellow), K8 (green), and α-SMA (red) on sequential tissue slices from hyperplastic mammary glands: 5-week-old Ddr2$^{lacZ/+}$; MMTV-PyMT mice. Scale bars, 50 μm.

(D) Dual in situ hybridization for mRNA (left) of 13-week primary breast tumor slices from Ddr2$^{+/+}$; MMTV-PyMT mice. K14 (red) and DDR2 (green) stain in the top panels and K8 (red) and DDR2 (green) stain in the bottom panels. White arrows on H&E-stained images (right) identify cells expressing both transcripts. Scale bars, 50 μm.

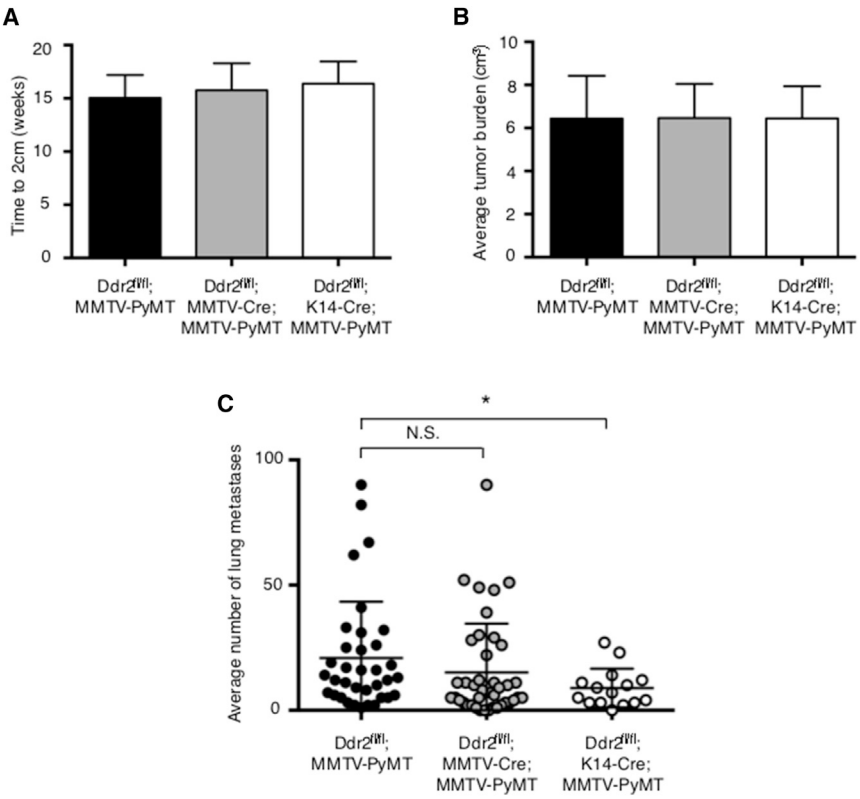

Figure 4. DDR2 Deletion in Basal, but Not Luminal, Breast Epithelial Cells Inhibit Lung Metastasis

(A) Primary tumor growth rates in indicated mice, determined by the age at which the largest tumor reached 2 cm in diameter. 15–35 mice per group. Data are presented as mean ± SD.

(B) Total tumor burden of indicated mice, determined by the sum of the volume of all tumors for each mouse when the largest tumor reached 2 cm in diameter. Tumor volumes were calculated by $V = 0.52 \cdot (W^2) \cdot L$. 15–35 mice per group. Data are presented as mean ± SD.

(C) Quantification of lung metastases in indicated mice presented as the average number of microscopically visible metastases counted from three H&E-stained sections of lung from each mouse taken 200 μm apart, normalized to the total lung area. *$p < 0.01$; N.S., not significant. 15–35 mice per group. Data are presented as mean ± SD.

growth or total primary tumor burden for either Cre transgene (Figures 4A and 4B). Surprisingly, in mice in which DDR2 was deleted using MMTV-Cre, there was no significant effect on the number of lung metastases (Figure 4C). In contrast, when DDR2 was deleted with K14-Cre, there was a statistically significant reduction in lung metastasis, but not to the level observed when Ddr2 was ubiquitously deleted (Figure 4C versus Figure 2C).

These disparate results were unexpected, as MMTV-PyMT tumors develop from luminal mammary epithelial cells. Since the $Ddr2^{fl/fl}$ allele was in a mixed C57BL/6/FVBn background, this could account for the observed difference in metastatic phenotypes between MMTV-Cre- and K14-Cre-deleted Ddr2. To address this, we analyzed the number of lung metastases according to the percentage of FVB/n background (Figures S3A–S3C). The results were consistent, regardless the degree of backcrossing to FVB/n, showing a statistically insignificant reduction of lung metastasis when DDR2 was deleted in the MMTV-Cre line. Another possibility could be that MMTV-Cre expression was less efficient than K14-Cre. To test this, we measured the recombination of the conditional allele by PCR in mouse endothelial cells (MECs) isolated from MMTV-Cre, $Ddr2^{fl/fl}$ and K14-Cre, $Ddr2^{fl/fl}$ mice (Figure S3D). In both lines, over 90% of the DDR2 gene was recombined compared to $Ddr2^{fl/fl}$ control. MMTV-Cre and K14-Cre expression patterns were further confirmed, using the ROSA-LSL-TdTomato reporter allele (Madisen et al., 2010). In normal adult mammary glands, there was luminal expression of Tomato in MMTV-Cre mice, and luminal and basal expression in K14-Cre mice, as anticipated (Figures S3E–S3G). MMTV-Cre and K14-Cre expression in breast tumors showed that all MMTV-PyMT tumors expressed Tomato. All lung metastatic foci identified in H&E-stained sections from both MMTV-Cre and K14-Cre mice were also Tomato positive (Figure S3F).

In sum, these analyses demonstrated that the loxP sites were functional in vivo and that expression of both MMTV-Cre and K14-Cre was efficient and equivalent. Thus, differences in MMTV-Cre and K14-Cre expression likely did not explain the difference in metastatic phenotype.

Action of DDR2 in Cells within the Tumor Environment Is Also Important for Breast Cancer Metastasis

Selective deletion of DDR2 in breast epithelial cells (K14-Cre) did not inhibit lung metastasis to the same extent as when DDR2 was ubiquitously deleted. This raised the possibility that the action of DDR2 in cells within the tumor stroma or environment may also contribute to breast cancer metastasis. To determine whether this is the case, we performed reciprocal transplant experiments using primary breast tumor cells isolated from $Ddr2^{+/+}$; MMTV-PyMT or $Ddr2^{-/-}$; MMTV-PyMT mice that were implanted into the mammary fat pads of syngeneic $Ddr2^{+/+}$ or ubiquitous $Ddr2^{-/-}$ recipient mice. Regardless of tumor or host Ddr2 genotype, transplanted primary breast tumors reached 2 cm in diameter between 6 and 10 weeks post-implantation (Figure 5A). Histological analysis of lungs once primary breast tumor reached 2 cm revealed lung metastases in control $Ddr2^{+/+}$ recipients transplanted with $Ddr2^{+/+}$ tumor cells (Figure 5B). WT Ddr2 recipients of $Ddr2^{-/-}$ tumor cells had reduced lung metastases consistent with a role for DDR2 in tumor cells (Figure 5B). However, interestingly, when $Ddr2^{-/-}$ mice were transplanted with $Ddr2^{+/+}$ tumor cells, lung metastases were dramatically inhibited as well (Figure 5B). This indicated that the action of DDR2 within cells of the host tumor environment also contributed to DDR2's ability to regulate breast cancer metastasis.

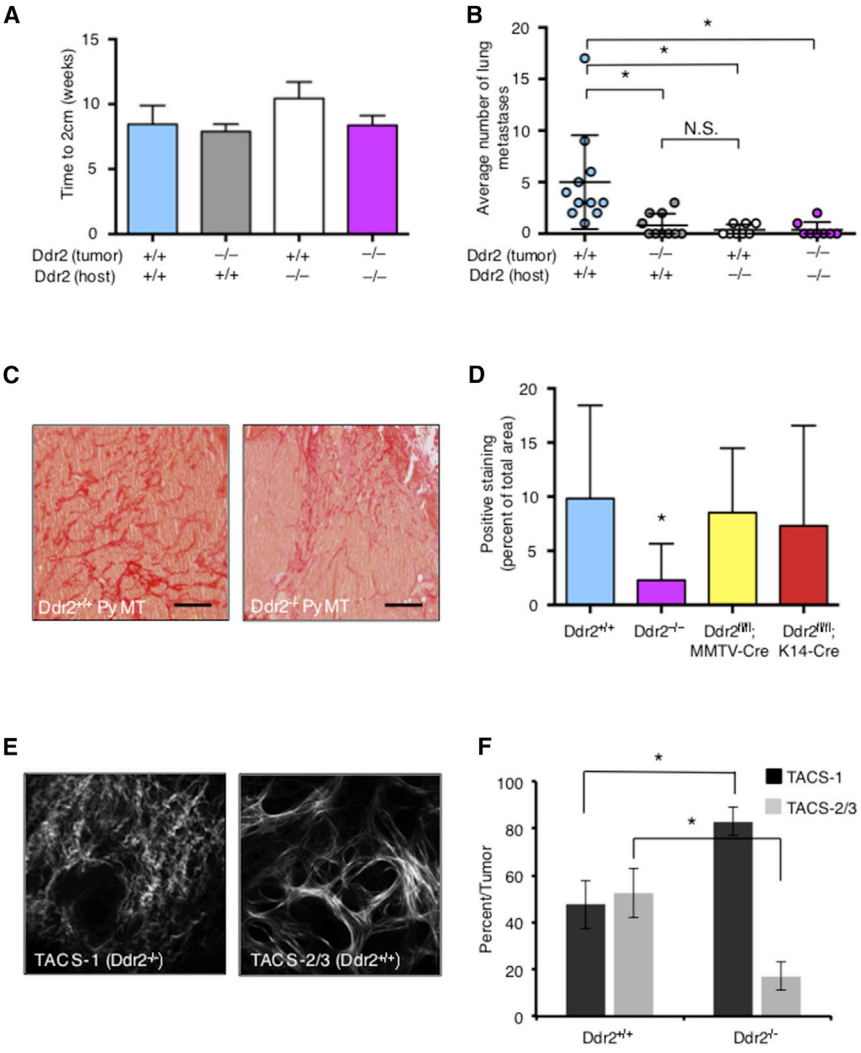

Figure 5. The Action of DDR2 in the Tumor Stroma Is Critical for Metastasis

(A and B) Reciprocal transplant of MMTV-PyMT primary tumors cells from the indicated genotypes were transplanted into the breasts of syngeneic (FVBn) hosts of the indicated genotype. Time to the development of a 2-cm breast tumor was scored (A). 8–11 mice per group. Quantification of lung metastases as the average number of microscopically visible metastases counted from three H&E-stained sections of lung from each mouse taken 200 μm apart normalized to the total lung area (B). *$p < 0.01$; N.S., not significant. 8–11 mice per group. Data are presented as mean ± SD.

(C) Picrosirius red staining on tumor sections from $Ddr2^{+/+}$; MMTV-PyMT and ubiquitous $Ddr2^{-/-}$; MMTV-PyMT mice. Scale bars, 100 μm.

(D) Quantification of Picrosirius red staining from (C). Positive staining was calculated as the percentage of red pixels over the total number of pixels in the image. *$p < 0.001$. Data are presented as mean ± SD.

(E) Representative second-harmonic-generation images of collagen organization in 10- to 13-week tumors from $Ddr2^{+/+}$ and ubiquitous $Ddr2^{-/-}$ mice. Curly collagen fibers (left image) were scored as TACS-1, and straight collagen fibers (right image) were scored as TACS-2/3.

(F) Percentage of images scored as TACS-1 or TACS-2/3 from $Ddr2^{+/+}$ PyMT tumors and $Ddr2^{-/-}$ PyMT tumors. Three 13-week and four 10-week mice of each genotype were analyzed. Three or four tumors from each mouse were isolated, and three to four images from each tumor were acquired. Total of 77 images scored. Student's t test, *$p < 0.05$. Data are presented as mean ± SD.

Ubiquitous Deletion of DDR2 in Breast Tumors Is Associated or Correlated with Less Advanced or Aggressive Primary Tumors

To determine how the action of DDR2 in tumor and tumor stromal cells could impact the primary tumor environment, we performed Picosirius Red staining to assess the extent of fibrillar collagen deposition. MMTV-PyMT primary tumors are typically highly fibrotic, and increased fibrillar collagen deposition within primary tumors is a poor prognostic factor. In ubiquitous $Ddr2^{-/-}$; MMTV-PyMT primary tumors, there was significant reduction in total fibrillar collagen (Figure 5C; quantified in Figure 5D), whereas primary breast tumors from $Ddr2^{fl/fl}$; MMTV-Cre; MMTV-PyMT and $Ddr2^{fl/fl}$; K14-Cre; MMTV-PyMT mice did not show a reduction in fibrillar collagen levels (Figure 5D).

Certain features about collagen architecture within the tumor stroma (e.g., fiber orientation, thickness, linearity) are associated with poor clinical outcomes. Collagen fiber structure in primary breast tumors was assessed by second-harmonic generation (SHG) microscopy on tissue sections from 10- to 13-week tumors. Multiple primary breast tumors per mouse from multiple mice were scored for their TACS, as described previously (Provenzano et al., 2006). $Ddr2^{+/+}$; MMTV-PyMT tumors exhibited predominantly TACS2/3 scores (more linear, thicker collagen fibers), consistent with aggressive and invasive tumors (Figure 5E; quantified in Figure 5F). In contrast, age-matched ubiquitous $Ddr2^{-/-}$; MMTV-PyMT tumors exhibited predominantly a TACS1/2 score (curly collagen fibers) that is associated with less aggressive tumors (Figure 5E; quantified in Figure 5F).

Increased primary tumor vasculature can promote tumor cell invasion and metastatic disease (Moserle and Casanovas, 2013). $Ddr2^{+/+}$; MMTV-PyMT tumors were found to have significantly higher CD31 staining than that of ubiquitous $Ddr2^{-/-}$; MMTV-PyMT tumors (Figure S4A; quantified in Figure S4B). Another major constituent of the tumor stroma are immune cells, which can promote or inhibit tumor progression and invasion (Grivennikov et al., 2010). We enumerated immune cell infiltrates in $Ddr2^{+/+}$; MMTV-PyMT and ubiquitous $Ddr2^{-/-}$; MMTV-PyMT primary breast tumors and found no difference in the number of immune cells in 13-week and 20-week primary tumors (Figures S4C–S4H).

Histologic comparison of $Ddr2^{+/+}$ and ubiquitous $Ddr2^{-/-}$ primary tumors (at 10 weeks) revealed significantly less advanced carcinomas in $Ddr2^{-/-}$ tumors (Figures S5A and S5B; quantified

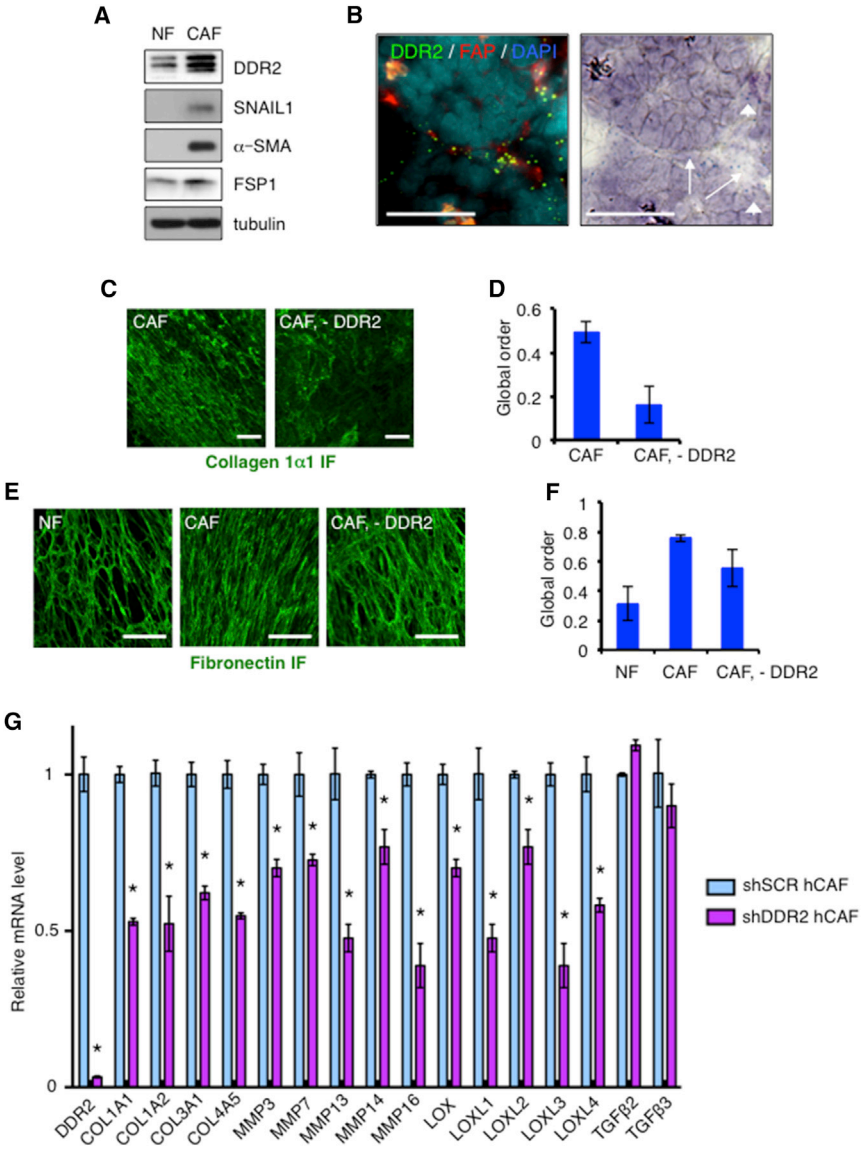

Figure 6. The Action of DDR2 in CAFs Regulates Production of Tumor-Associated ECM

(A) Western blot for DDR2, SNAIL1, α-SMA, and FSP1 proteins in normal human breast fibroblasts or human breast CAFs.

(B) Dual in situ hybridization for mRNA (left) of 13-week primary breast tumor slices from Ddr2$^{+/+}$; MMTV-PyMT mice. FAP (red) and DDR2 (green). White arrows on H&E-stained images (right) identify cells within the tumor stroma that express both transcripts. White arrowheads identify tumor cells expressing DDR2 mRNA. Scale bars, 50 μm.

(C) Immunofluorescence staining for collagen 1α1 matrix produced by mouse breast tumor CAFs. Scale bars, 50 μm.

(D) Quantification of global fiber alignment in (C). Data are presented as mean ± SD.

(E) Immunofluorescence staining for fibronectin matrix produced by normal human mammary fibroblasts (left), human breast tumor CAFs (control SCR shRNA; middle), or hCAFs depleted of DDR2 by shRNA (right). Scale bars, 50 μm.

(F) Quantification of global fiber alignment in (E). Data are presented as mean ± SD.

(G) qPCR analysis of mRNA isolated from human CAFs, short hairpin (sh) RNA (shRNA) depleted of DDR2, or transduced with scrambled control (SCR). Multiple replicates of each gene were performed for each experiment. Data are representative of two independent experiments. Data are presented as mean ± SD. *p < 0.01.

in Figure S5C). It should be noted, however, that this histologic difference was not apparent in 14-week and terminal (18- to 20-week) tumors, likely because at this time point in tumor progression they are so advanced, occupying almost the entire breast tissue. Despite the presence in Ddr2$^{-/-}$ primary tumors of numerous histologic features associated with less aggressive or invasive tumors (e.g., decreased fibrosis, decreased angiogenesis, and more benign stromal TAC signature), we did not detect a difference in the number of circulating tumor cells (CTCs) between Ddr2$^{+/+}$ and Ddr2$^{-/-}$ tumor-bearing mice (Figures S5D and S5E). This may reflect the wide variance in results per mouse or that reliable detection of CTC required analyzing mice at the terminal stage of breast tumor development (18- to 20-week tumors in PyMT and 2-cm tumor in the 4T1 transplant model) when primary tumors in both Ddr2$^{+/+}$ and Ddr2$^{-/-}$ mice all exhibit advanced carcinoma.

When considered in the aggregate, these analyses of Ddr2$^{-/-}$ primary breast tumors were mostly associated with or correlated with less advanced or aggressive primary tumors suggesting that the action of DDR2 in the primary tumor (tumor cells and tumor stromal cells) affected metastasis.

The Action of DDR2 in CAFs Is Critical for Production of Tumor-Associated ECM

In contrast to tumors ubiquitously deleted of DDR2, selective deletion of DDR2 in breast epithelial cells (MMTV-Cre or K14-Cre) was not associated with any change in tumor matrix collagen (Figure 5D). This implicates the action of DDR2 in tumor stromal cells as responsible for observed changes in tumor matrix or collagen fibers. Knowing that CAFs are the major source of collagen production in breast tumors (Bhowmick et al., 2004) and that DDR2 was expressed by CAFs, we asked whether the action of DDR2 in CAFs affected ECM production and remodeling. We isolated and purified primary CAFs from DDR2$^{+/+}$ and ubiquitous DDR2$^{-/-}$ mouse PyMT breast tumors as well as depleted DDR2 from human breast tumor CAFs with specific short hairpin (sh)DDR2 RNAi.

DDR2 expression was increased in breast CAFs compared to normal breast fibroblasts (Figure 6A). ISH analysis of Ddr2$^{+/+}$; MMTV-PyMT tumors revealed that DDR2 mRNA was expressed in FAP+ CAFs (Figure 6B). WT CAFs produced a highly aligned, or ordered, collagen I and fibronectin matrix (Figures 6C and 6E). Depletion of DDR2 led to a significant change in the global order

of the ECM fibers, producing an ECM similar to that of normal mammary fibroblasts (Figure 6E). The degree of global order of matrix fibers was measured using a sub-window 2D Fourier transform method (Figures 6D and 6F; Figures S5F–S5I) (Cetera et al., 2014; Sander and Barocas, 2009). Real-time qPCR analysis of select fibrogenic gene expression by WT and Ddr2$^{-/-}$ CAFs revealed a significant reduction in the expression of several collagen genes, collagen-modifying genes (lysyl oxidases; LOX), and matrix-remodeling enzymes (metalloproteinases; MMPs) in CAFs depleted of DDR2 (Figure 6G).

These data demonstrated that the action of DDR2 in CAFs is critical for ECM production and remodeling. When coupled with SHG analysis of collagen fibers in primary tumors, this indicated that the action of DDR2 in tumor CAFs, and possibly other stromal cells, is critical for production of the tumor stromal ECM.

The Action of DDR2 in Both K14+ Tumor Cells and Tumor Stromal CAFs Is Critical for Collective Invasion/Migration of Primary Tumor Organoids

Tumor-cell-based culture studies (in 2D and 3D) have described a critical role for DDR2 in regulating tumor cell invasion and migration (Zhang et al., 2013). K14+ cells within breast tumors are thought to lead collective invasion of tumor cells (Cheung et al., 2013). Thus, we hypothesized that the decrease in lung metastasis in ubiquitous Ddr2$^{-/-}$ and K14-Cre-deleted DDR2 tumors was a result of reduced collective invasion regulated by K14+ tumor cells. To test this, we utilized a tumor organotypic 3D culture system (Nguyen-Ngoc et al., 2012). To model normal breast epithelial environment, tumor organoids were cultured in 3D Matrigel, while to model the stromal matrix invading/migrating tumor cells encounter, tumor organoids were cultured in 3D collagen I gels. In these culture systems, K14+ tumor cells acquire leader cell behavior when tumor organoids are cultured in 3D collagen I gels and give rise to invasive protrusions (Cheung et al., 2013).

When primary tumor organoids from Ddr2$^{+/+}$ and Ddr2$^{-/-}$ mice were plated on normal tissue culture plates (2D cultures), both grew in cobblestone islands characteristic of epithelial cells (Figure S6A), and there was no change in proliferation rates between them (Figure S6B). In collagen I gels, there was a dramatic reduction in the number of invasive tumor organoids present when DDR2 was deleted in all cells within the tumor or with K14-Cre, but not MMTV-Cre (Figure 7E). In Matrigel, tumor organoids from ubiquitous Ddr2$^{-/-}$; MMTV-PyMT tumors exhibited reduced budding and branching, while deletion of DDR2 in tumor cells with either MMTV-Cre or K14-Cre had no effect on tumor organoid budding and branching (Figure S6C; quantified in Figure S6D).

A trivial explanation for the effect of DDR2 gene deletion upon tumor organoid invasiveness could be that DDR2 affects K14+ cell fate; thus, fewer K14+ leader cells are present. However ubiquitous absence of DDR2 did not affect the number of K14+ tumor cells per tumor organoid compared to WT tumor organoids (Figure S6E; quantified in Figure S6F). We also analyzed Ddr2$^{-/-}$ primary tumors for any change in the level of α-SMA, K8, and K14 staining. We did not observe any differences in the numbers of these cell populations between Ddr2$^{+/+}$; MMTV-PyMT and Ddr2$^{-/-}$; MMTV-PyMT primary breast tumor (Figures S7A–S7F).

Tumor organoids contain not only tumor cells but also tumor stromal cells such as CAFs, and CAFs can influence tumor cell invasiveness through paracrine mechanisms, ECM production, and ECM remodeling. IF analysis with anti-FAP antibodies revealed that 23% of WT tumor organoids contain FAP^{+} cells (CAFs) (Figure S6G; quantified in Figure S6H) and that all FAP+ cells were located at the tumor-stromal boundary of tumor organoids.

To determine whether the action of DDR2 in CAFs influenced paracrine functions of CAFs that support or enhance collective tumor cell invasion in collagen I gels, we performed mixing studies. Addition of WT CAFs to WT MMTV-PyMT tumor organoids increased the number of invasive tumor organoids detected (Figure 7B versus Figure 7C; quantified in Figure 7E). This effect required the presence of DDR2 in CAFs, as when DDR2$^{-/-}$ CAFs were added to WT tumor organoids, there was no change (increase or decrease) in the number of invasive tumor organoids (Figure 7C versus Figure 7D; quantified in Figure 7E). K14-Cre-deleted DDR2 tumor organoids, but not MMTV-Cre-deleted DDR2 tumor organoids, also exhibited a dramatically reduced number of invasive colonies (equivalent to ubiquitous Ddr2$^{-/-}$ tumor organoids) (Figure 7E). Surprisingly, the addition of WT CAFs to ubiquitous Ddr2$^{-/-}$ tumor organoids and K14-Cre-deleted DDR2 tumor organoids rescued the invasive phenotype, but only to the level observed with WT tumor organoids alone, not to the level of WT tumor organoids plus WT CAFs (Figure 7E). This effect was DDR2 dependent, as the addition of Ddr2$^{-/-}$ CAFs did not rescue invasiveness of either ubiquitous Ddr2$^{-/-}$- or K14-Cre-deleted DDR2 tumor organoids.

These analyses revealed a tumor cell-intrinsic function of DDR2 in K14+ cells that influenced collective cell invasion/migration of tumor organoids in 3D collagen I gels. In addition, the action of DDR2 in CAFs influenced collective invasiveness of primary breast tumor organoids through a signaling pathway (or pathways) in tumor cells distinct from the tumor-cell-intrinsic function of DDR2.

DISCUSSION

We have demonstrated that the action of the collagen receptor DDR2 in both tumor cells and tumor stromal cells within the primary tumor environment is critical for breast cancer metastasis in genetically engineered mouse models (GEMMs) of cancer. We also observed that the action of DDR2, a receptor tyrosine kinase, did not influence growth or proliferation of primary tumors in vivo. We have identified three cellular functions for DDR2 within cells within the primary tumor: (1) In K14+ tumor cells, DDR2 plays a cell-intrinsic role regulating tumor collective migration. (2) In CAFs, the action of DDR2 is critical for the production and remodeling of the tumor matrix ECM. (3) Also, in CAFs, the action of DDR2 provides a signal that positively influences tumor collective migration, and this signal is distinct from DDR2's tumor cell-intrinsic regulation of tumor collective migration.

Despite inhibiting collective cell invasion and migration of primary tumor organoids in collagen I and epithelial branching in Matrigel, we did not observe any defect in mammary gland

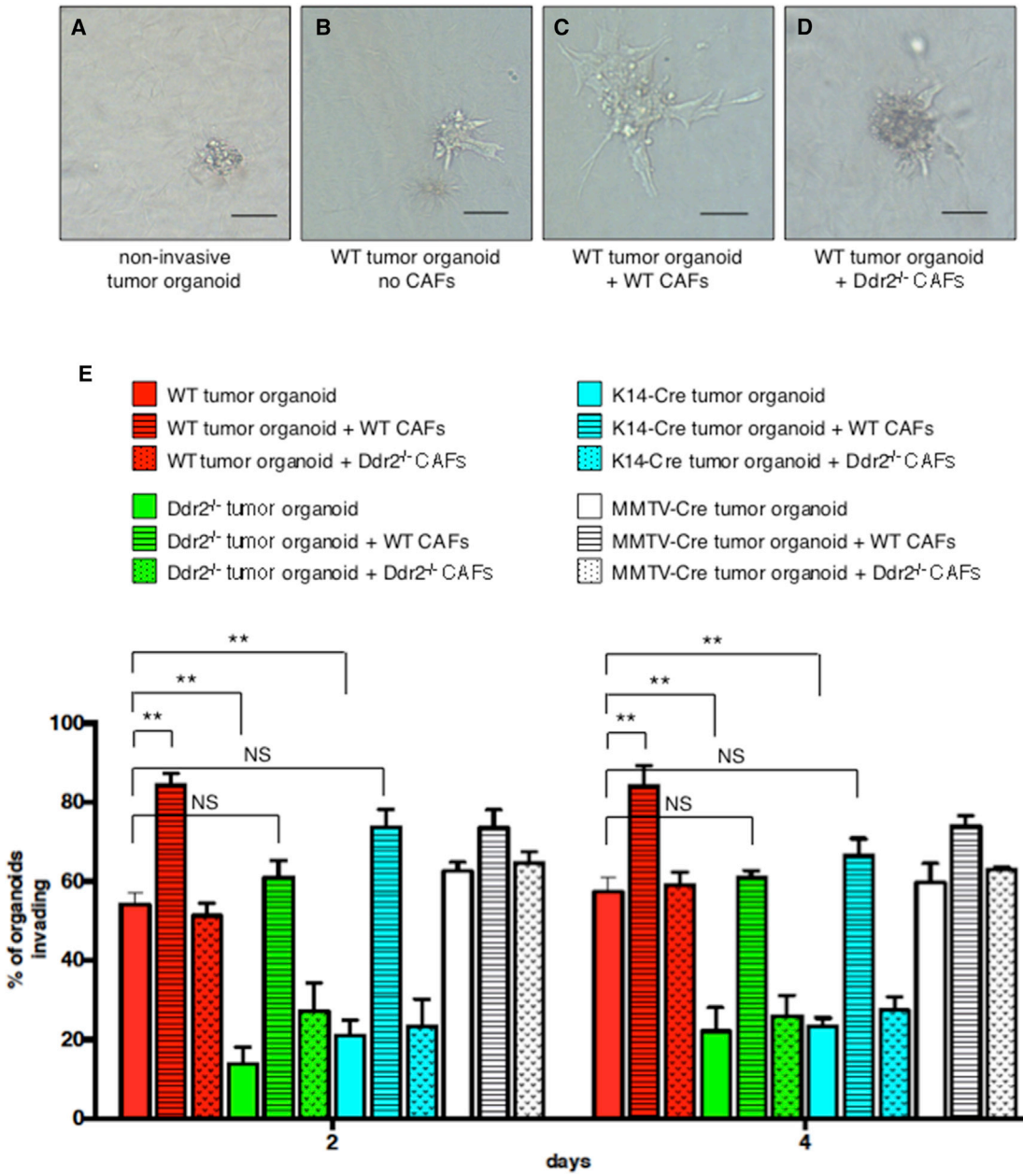

Figure 7. Action of DDR2 in K14$^+$ Tumor Epithelial Cells and CAFS Regulate Collective Invasion by Primary Tumor Organoids

(A-D) Representative images of tumor organoids scored. (A) Non-invasive tumor organoid, no added CAFs. (B) Invasive WT tumor organoid, no added CAFs. (C) Invasive WT tumor organoid cultured in the presence of WT breast CAFs. (D) Invasive WT tumor organoid cultured in the presence of Ddr2$^{-/-}$ breast CAFs. Scale bars, 100 μm.

(E) Quantification of number of invasive tumor organoids as a percentage of total organoids scored. In each well, 30 organoids were scored. All experimental conditions were performed in triplicate. The experiment was performed three separate times. **$p < 0.001$; NS, no significant difference.

Data are presented as mean ± SD.

morphogenesis during the development of Ddr2$^{-/-}$ mice. This may be explained by the observation that DDR2 is not expressed in normal mammary ECs.

Within tumor cells, the action of DDR2 was not required in luminal cells. However, deletion of DDR2 driven by K14-Cre had a significant effect on tumor metastasis in vivo and migration in 3D collagen I. Although MMTV-Cre deletes DDR2 in luminal cells, K14-Cre deletes DDR2 in luminal and basal cells (Figure S3G) (Van Keymeulen et al., 2011; Mitchell and Serra, 2014). DDR2 might need to be deleted in both populations to affect significant reduction in lung metastasis. It is also possible that the cells critical for metastasis spread are the K14+ cells.

Recent work has identified K14+ cells as leader cells critical for collective invasion/migration in vitro and in human breast cancers (Cheung et al., 2013). It has also been shown that the cells leading the collective migration are derived from the bulk of the tumor by expressing a set of basal genes, including K14 (Cheung et al., 2013). In the context of the MMTV-PyMT, K14-Cre, $Ddr2^{fl/fl}$ mice, this suggests that DDR2 would be deleted in all the cells that are leading migration. This might indicate that the action of DDR2 is required only in the K14+ epithelial cells and suggest that the tumor-cell-intrinsic role for DDR2 was predominantly to control tumor cell collective invasion/migration by K14+ leader cells. MMTV-PyMT, K14-Cre, $Ddr2^{fl/fl}$ tumor organoids showed reduced invasion in collagen I (Figure 7E) but no significant reduction of branching in Matrigel (Figures S6C and S6D). Since it has been suggested that the K14+ cells acquire leader cell behaviors specifically in collagen I microenvironments (Cheung et al., 2013), this might indicate that DDR2 role in K14+ is important mostly in leader cells in the collagen-I-rich tumor stromal environment.

The action of DDR2 in K14+ tumor cells was critical for the invasive program of primary tumor organoids in 3D collagen I gels. DDR2 signals could regulate tumor cell collective invasion in K14+ cells by stabilizing the EMT factor SNAIL1, thereby maintaining an invasive EMT phenotype (Zhang et al., 2013). Whether the action of DDR2 in leader K14+ basal-like tumor cells requires SNAIL1 or is independent of SNAIL1 remains to be determined, but it has been argued that the invasive program of primary tumor organoids can occur independently of some EMT factors and that tumor cells remain E-cadherin positive (Cheung et al., 2013). However, increasing evidence supports the plasticity of the EMT phenotype and, therefore, tumor cells may exist in dynamic partial epithelial or mesenchymal states (Savagner, 2015). In the PyMT breast tumor model, virtually all primary breast tumors are SNAIL1 positive (Tran et al., 2014), so it remains to be determined whether DDR2 has as dramatic an effect upon metastasis in other mouse models of breast cancer where expression of SNAIL1 is not as prevalent. Recent IHC analysis of human breast cancers found high levels of DDR2 associated with high tumor grade, triple-negative breast cancer (TNBC), and worse survival (Toy et al., 2015). TNBC of the basal or claudin-low subtypes are more likely to express SNAIL1.

A common feature of primary breast tumors is an increased abundance of ECM deposition (especially fibrillar collagens), which, when present, is associated with increased risk of invasive disease and shorter patient survival (Walker, 2001; Kreike et al., 2007). MMTV-PyMT mouse breast tumors are typically fibrotic, and ubiquitous DDR2 deletion led to significant reduction in the amount of fibrillar collagen and benign-appearing collagen fiber architecture. Reciprocal transplant experiments demonstrated that the action of DDR2 in the tumor environment was also critical for breast cancer metastasis. DDR2 has been implicated in the cellular synthesis and remodeling of fibrillar collagens within the ECM (Ferri et al., 2004; Sivakumar and Agarwal, 2010; Zhang et al., 2013), collagen 1α1 transcription (Zhang et al., 2013), and the expression and activation of matrix metalloproteinases (Leitinger, 2014). DDR2 expression has also been shown to be increased in bleomycin-induced lung fibrosis and CCl_4-induced hepatic fibrosis (Olaso et al., 2011; Yang et al., 2013). All of these reports lend support to the notion that DDR2 activation promotes collagen production or remodeling in tumors. CAFs are the main producers of ECM proteins and ECM remodeling enzymes (Bhowmick et al., 2004), DDR2 expression is activated in CAFs, and depletion of DDR2 in CAFs results in less ECM production and altered collagen architecture—features correlated with tumor cell invasion and metastasis. Furthermore, $Ddr2^{-/-}$ CAFs do not support invasion of tumor organoids in collagen I. In sum, these observations implicate the action of DDR2 in CAFs within the primary tumor as being critical for regulation of breast cancer metastasis.

DDR2-positive CAFs could arise from tumor cell EMT, but DDR2 is also expressed by normal human breast fibroblasts, and expansion of resident fibroblasts is thought to be the largest source of CAFs in tumors. Tumor cells and other stromal cells (e.g., immune cells) could also influence collagen production by CAFs, as factors secreted by these cells, or factors released from ECM remodeling, can stimulate collagen production and may be lacking in $Ddr2^{-/-}$ cells (Walker, 2001; Kalluri and Zeisberg, 2006).

Another environmental aspect influencing tumor cell invasion is physical stiffness of the ECM. Increased deposition of ECM proteins not only changes the biochemical signals that tumor cells encounter but also changes the physical environment in which they grow and migrate (Schedin and Keely, 2011). Increasing matrix stiffness promotes local invasion of mammary epithelial organoids and enhances tumor cell migration, predominantly through the Rho-ROCK pathway downstream of integrins (Paszek et al., 2005; Schedin and Keely, 2011). Since $Ddr2^{-/-}$; MMTV-PyMT primary tumors have significantly less fibrillar collagen and the fibers are less linear and thick than $Ddr2^{+/+}$; MMTV-PyMT tumors, it is possible that the tumor tissue is less stiff, thereby also contributing to decreased tumor cell invasion and migration.

Integrin activity in tumors is clearly critical for breast cancer metastasis (Seguin et al., 2015). Thus, it is remarkable that genetic deletion of DDR2, in the presence of integrins, has such a dramatic effect upon metastasis. In cells in culture, DDR2 can be activated by fibrillar collagens, even when β1-integrins are inhibited (Zhang et al., 2013). DDR2, itself, is a poor adhesive molecule yet can mildly affect integrin activity in cells (Xu et al., 2012). Therefore, it remains a possibility that DDR2-integrin crosstalk is important for tumor cell invasion or metastasis in vivo.

Although we did not see significant changes in the numbers of specific immune cell types in the primary tumors of $Ddr2^{+/+}$; MMTV-PyMT and $Ddr2^{-/-}$; MMTV-PyMT mice, it is possible that DDR2 loss could lead to changes in immune cell function. DDR2 is expressed in neutrophils and required for neutrophil migration through 3D collagen matrices (Afonso et al., 2013). DDR2 also plays a role in the collagen-induced activation of dendritic cells (Lee et al., 2007) and is expressed in macrophages in atherosclerotic lesions (Ferri et al., 2004), but little else is known about the function of DDR2 in immune cells, particularly in tumors. We cannot exclude the possibility that another subset of immune cells has a role in DDR2-mediated breast cancer metastasis.

It has been reported that DDR2 is expressed in tumor-associated human ECs and promotes the angiogenic capacity of ECs (Zhang et al., 2014). Syngeneic transplant experiments demonstrated a reduction in angiogenesis when B16-F10 melanoma tumors were subcutaneously implanted into DDR2-null mice, and these tumors had reduced mRNA levels of pro-angiogenic factors such as Vegfr2 and Ang-2. We also observed a significant reduction in blood vessel growth in Ddr2$^{-/-}$; MMTV-PyMT primary tumors. Therefore, DDR2 may promote metastasis, in part, by stimulating blood vessel growth in primary tumors or through regulating factors secreted by tumor or other stromal cells that regulate angiogenesis.

In summary, our data may explain, in part, why patients with primary breast tumors that have high levels of fibrillar collagen deposition are associated with invasive and metastatic disease and poorer outcomes. These studies argue that DDR2, a unique receptor tyrosine kinase, could be an important therapeutic target in breast cancer metastasis and that treatments selectively targeting DDR2 would impact both tumor cells and tumor environment simultaneously.

EXPERIMENTAL PROCEDURES

For more information, see the Supplemental Information.

Generation of Modified Ddr2 Alleles

Embryonic stem cells containing the targeted Ddr2 allele (Ddr2$^{tm1a(EUCOMM)Wtsi}$) were obtained from EUCOMM and injected into C57BL/6 tetraploid embryos. Founder mice were crossed to β-actin-Cre mice or FLP^{O} mice to generate Ddr2$^{lacZ/+}$ or Ddr2$^{fl/+}$ alleles, respectively. Ubiquitous Ddr2-null mice (Ddr2$^{null/null}$, Ddr2$^{lacZ/lacZ}$ and Ddr2$^{-/-}$) were backcrossed at least six generations onto a pure FVB/N background. Conditional Ddr2$^{fl/fl}$ mice were on a mixed FVBN/C57BL/6 background. All mice were used in compliance with the Washington University Institutional Animal Care and Use Committee under protocol #21020142.

Mouse Tumor Studies

Both ubiquitous and conditional Ddr2$^{-/-}$ mice were crossed to MMTV-PyMT mice. Conditional Ddr2$^{fl/fl}$ mice were crossed to K14-Cre (Jackson Laboratory, stock #004782), MMTV-Cre, and ROSA-LSL-TdTomato mice. Tumor-bearing mice were monitored weekly and euthanized when the largest tumor reached 2 cm in diameter. Mammary gland transplants were performed as previously described (Zhang et al., 2013).

Analysis of Lung Metastasis

Lungs were fixed overnight in 10% formalin, then washed with 70% ethanol, and processed and embedded in paraffin blocks. Tissue sections (5 μm) were stained with H&E. Microscopically visible metastatic foci were counted from three sections taken 200 μm apart and reported as the average number of metastases per section.

SHG Image Acquisition and Analysis

Tumors from 10- to 13-week-old animals were fixed in 10% neutral buffered formalin overnight. Collagen matrix images were observed using multiphoton laser scanning microscopy (MPLSM) and SHG on a Bruker IV multiphoton microscope tuned to a wavelength of 890 nm. Images were focused onto a Zeiss 20× Plan Apo water-immersion lens (numerical aperture, 1.0), and SHG emission was observed at 445 nm and discriminated from fluorescence using a 445-nm emission filter with a 20-nm narrow bandpass. Three to four 20-μm z stacks were collected with a 2-μm step size for each tumor (43 z stacks represent 11 tumors from six Ddr2+/+ mice, and 34 z stacks represent 9 tumors from five Ddr2$^{-/-}$ mice). The z stacks were compressed into one image, and collagen fiber organization was scored by three blinded reviewers as TACS-1 (curly fibers) or TACS-2/3 (straight fibers), as described previously (Provenzano et al., 2006). The majority score was used for each image, percent TACS-1 versus TACS-2/3 score was determined for each tumor, and the average percent score was determined for Ddr2$^{+/+}$ versus ubiquitous Ddr2$^{-/-}$.

Isolation and Culture of Primary Tumor Cells and Tumor Organoids

Mouse mammary tumor organoids were isolated as previously described (Nguyen-Ngoc et al., 2012). Primary tumor organoids (30–50, each ~200–1,000 cells) with or without CAFs (750) were cultured in 50-μl droplets of either growth-factor-reduced Matrigel or 3 mg/ml acid-solubilized rat-tail collagen I (BD Biosciences). Alternatively, organoids were plated on normal tissue culture plates to expand the cells and perform experiments with single cells (transplants, transwell assay, proliferation analysis). Immunofluorescence quantification of organoids was performed by measuring the ratio of fluorescein isothiocyanate (FITC) to DAPI signal intensity within annular regions of interest extending from the organoid surface to 17 μm (50 pixels) into the organoid to focus on expression in the outermost layer of cells. These regions of interest were identified using automated intensity and distance thresholding implemented in a custom MATLAB program.

Isolation of CAFs

MMTV-PyMT tumors were dissected and minced, and minced pieces were transferred to ~20 ml of digestion media per tumor (DMEM, 1% fetal bovine serum [FBS], 0.2% collagenase A (Roche), 0.2% trypsin (GIBCO 27250-018), 50 μg/ml gentamycin, 5 μg/ml insulin) and rocked at 37°C for 30–45 min. The digested tissue was then washed twice with serum-free media and treated with DNase for 5 min at room temperature. Tissue was resuspended in ice-cold serum-free media and serially centrifuged four times. Single-cell fractions were collected and plated for 25–30 min in DMEM, 10% FBS at 37°C, 5% CO_2, 20% O_2. CAFs adhered to the plate, whereas other cells did not. The supernatant and non-adherent cells were removed, and CAFs were maintained in DMEM, 10% FBS at 37°C, 5% CO_2, 20% O_2 for 20+ passages, splitting one to two times per week. The immortalized primary cell lines were then submitted to fluorescence-activated cell sorting (FACS) with PDGFRα antibodies.

ECM Production by CAFs and Fibronectin and Collagen I Staining

Human CAFs were plated to confluence on 12-mm glass coverslips in DMEM supplemented with 10% FBS and 50 μg/ml ascorbic acid, and media were changed daily for 7 days. Cells were extracted on day 7 (25 mmol/l Tris-HCl [pH 7.4]; 150 mmol/l sodium chloride; 0.5% Triton X-100; and 20 mmol/l ammonia hydroxide) for 3–5 min. Cellular debris was carefully washed away with 1× PBS. Resultant cell-free ECMs were fixed in 4% paraformaldehyde for 15 min at room temperature and then blocked with 5% FBS in 1× PBS. ECMs were then incubated in mouse anti-fibronectin antibody (diluted 1:100; BD Biosciences) overnight at 4°C, washed twice, and then incubated in goat anti-mouse Alexa Fluor 488 secondary (diluted 1:500; Life Technologies), washed four times, mounted in Vectashield (VWR, 101098-044), and sealed with nail polish. IF was analyzed on a confocal microscope (LSM 700; Carl Zeiss) at room temperature with ZEN 2009 software. ImageJ was used to adjust brightness and contrast.

SUPPLEMENTAL INFORMATION

Supplemental Information includes Supplemental Experimental Procedures, seven figures, and three tables and can be found with this article online at http://dx.doi.org/10.1016/j.celrep.2016.05.033.

AUTHOR CONTRIBUTIONS

C.A.S.C. and G.D.L. conceived the project, designed the experiments, and wrote the manuscript. C.A.S.C. performed the majority of the experiments and data analysis. A.B. performed immune cell phenotyping, CTC analysis, and IF of tumor organoids. S.M.P. and Y.L. performed and analyzed the SHG imaging. K.Z. and S.V.H. isolated and performed the CAF analysis. S.V.H. performed the ISH experiments. A.J.L. quantified the CAF fiber global

alignment and assisted with the quantification of staining. D.G.D. performed histologic analysis of tumors. W.R.G. performed organoid and CAF mixing experiments. K.W.E., P.J.K., and G.D.L. supervised the research.

ACKNOWLEDGMENTS

This work was supported by the NIH grants F31 CA165729 (C.A.C.) and CA196205 (G.D.L.) and the Komen Foundation grant 110889 (G.D.L.). C.A.C. was also supported, in part, by NIH T32 training grant CA113275. We thank the Washington University Advanced Imaging and Tissue Analysis Core for tissue processing (NIH P30DK052574). We thank members of the G.D.L. lab for helpful discussions.

Received: April 16, 2015
Revised: March 15, 2016
Accepted: May 6, 2016
Published: June 2, 2016

REFERENCES

Afonso, P.V., McCann, C.P., Kapnick, S.M., and Parent, C.A. (2013). Discoidin domain receptor 2 regulates neutrophil chemotaxis in 3D collagen matrices. Blood *121*, 1644–1650.

Bhowmick, N.A., Neilson, E.G., and Moses, H.L. (2004). Stromal fibroblasts in cancer initiation and progression. Nature *432*, 332–337.

Boyd, N.F., Dite, G.S., Stone, J., Gunasekara, A., English, D.R., McCredie, M.R., Giles, G.G., Tritchler, D., Chiarelli, A., Yaffe, M.J., and Hopper, J.L. (2002). Heritability of mammographic density, a risk factor for breast cancer. N. Engl. J. Med. *347*, 886–894.

Cetera, M., Ramirez-San Juan, G.R., Oakes, P.W., Lewellyn, L., Fairchild, M.J., Tanentzapf, G., Gardel, M.L., and Horne-Badovinac, S. (2014). Epithelial rotation promotes the global alignment of contractile actin bundles during Drosophila egg chamber elongation. Nat. Commun. *5*, 5511.

Cheung, K.J., Gabrielson, E., Werb, Z., and Ewald, A.J. (2013). Collective invasion in breast cancer requires a conserved basal epithelial program. Cell *155*, 1639–1651.

Dassule, H.R., Lewis, P., Bei, M., Maas, R., and McMahon, A.P. (2000). Sonic hedgehog regulates growth and morphogenesis of the tooth. Development *127*, 4775–4785.

Ferri, N., Carragher, N.O., and Raines, E.W. (2004). Role of discoidin domain receptors 1 and 2 in human smooth muscle cell-mediated collagen remodeling: potential implications in atherosclerosis and lymphangioleiomyomatosis. Am. J. Pathol. *164*, 1575–1585.

Grivennikov, S.I., Greten, F.R., and Karin, M. (2010). Immunity, inflammation, and cancer. Cell *140*, 883–899.

Guy, C.T., Cardiff, R.D., and Muller, W.J. (1992). Induction of mammary tumors by expression of polyomavirus middle T oncogene: a transgenic mouse model for metastatic disease. Mol. Cell. Biol. *12*, 954–961.

Kalluri, R., and Zeisberg, M. (2006). Fibroblasts in cancer. Nat. Rev. Cancer *6*, 392–401.

Kano, K., Marín de Evsikova, C., Young, J., Wnek, C., Maddatu, T.P., Nishina, P.M., and Naggert, J.K. (2008). A novel dwarfism with gonadal dysfunction due to loss-of-function allele of the collagen receptor gene, Ddr2, in the mouse. Mol. Endocrinol. *22*, 1866–1880.

Kano, K., Kitamura, A., Matsuwaki, T., Morimatsu, M., and Naito, K. (2010). Discoidin domain receptor 2 (DDR2) is required for maintenance of spermatogenesis in male mice. Mol. Reprod. Dev. *77*, 29–37.

Kim, I.S., and Baek, S.H. (2010). Mouse models for breast cancer metastasis. Biochem. Biophys. Res. Commun. *394*, 443–447.

Kreike, B., van Kouwenhove, M., Horlings, H., Weigelt, B., Peterse, H., Bartelink, H., and van de Vijver, M.J. (2007). Gene expression profiling and histopathological characterization of triple-negative/basal-like breast carcinomas. Breast Cancer Res. *9*, R65.

Labrador, J.P., Azcoitia, V., Tuckermann, J., Lin, C., Olaso, E., Mañes, S., Brückner, K., Goergen, J.L., Lemke, G., Yancopoulos, G., et al. (2001). The collagen receptor DDR2 regulates proliferation and its elimination leads to dwarfism. EMBO Rep. *2*, 446–452.

Lee, J.E., Kang, C.S., Guan, X.Y., Kim, B.T., Kim, S.H., Lee, Y.M., Moon, W.S., and Kim, D.K. (2007). Discoidin domain receptor 2 is involved in the activation of bone marrow-derived dendritic cells caused by type I collagen. Biochem. Biophys. Res. Commun. *352*, 244–250.

Leitinger, B. (2014). Discoidin domain receptor functions in physiological and pathological conditions. Int. Rev. Cell Mol. Biol. *310*, 39–87.

Madisen, L., Zwingman, T.A., Sunkin, S.M., Oh, S.W., Zariwala, H.A., Gu, H., Ng, L.L., Palmiter, R.D., Hawrylycz, M.J., Jones, A.R., et al. (2010). A robust and high-throughput Cre reporting and characterization system for the whole mouse brain. Nat. Neurosci. *13*, 133–140.

Matsumura, H., Kano, K., Marín de Evsikova, C., Young, J.A., Nishina, P.M., Naggert, J.K., and Naito, K. (2009). Transcriptome analysis reveals an unexpected role of a collagen tyrosine kinase receptor gene, Ddr2, as a regulator of ovarian function. Physiol. Genomics *39*, 120–129.

Mitchell, E.H., and Serra, R. (2014). Normal mammary development and function in mice with Ift88 deleted in MMTV- and K14-Cre expressing cells. Cilia *3*, 4.

Moserle, L., and Casanovas, O. (2013). Anti-angiogenesis and metastasis: a tumour and stromal cell alliance. J. Intern. Med. *273*, 128–137.

Nguyen-Ngoc, K.V., Cheung, K.J., Brenot, A., Shamir, E.R., Gray, R.S., Hines, W.C., Yaswen, P., Werb, Z., and Ewald, A.J. (2012). ECM microenvironment regulates collective migration and local dissemination in normal and malignant mammary epithelium. Proc. Natl. Acad. Sci. USA *109*, E2595–E2604.

Olaso, E., Lin, H.C., Wang, L.H., and Friedman, S.L. (2011). Impaired dermal wound healing in discoidin domain receptor 2-deficient mice associated with defective extracellular matrix remodeling. Fibrogenesis Tissue Repair *4*, 5.

Paszek, M.J., Zahir, N., Johnson, K.R., Lakins, J.N., Rozenberg, G.I., Gefen, A., Reinhart-King, C.A., Margulies, S.S., Dembo, M., Boettiger, D., et al. (2005). Tensional homeostasis and the malignant phenotype. Cancer Cell *8*, 241–254.

Provenzano, P.P., Eliceiri, K.W., Campbell, J.M., Inman, D.R., White, J.G., and Keely, P.J. (2006). Collagen reorganization at the tumor-stromal interface facilitates local invasion. BMC Med. *4*, 38.

Provenzano, P.P., Inman, D.R., Eliceiri, K.W., Knittel, J.G., Yan, L., Rueden, C.T., White, J.G., and Keely, P.J. (2008). Collagen density promotes mammary tumor initiation and progression. BMC Med. *6*, 11.

Ren, T., Zhang, W., Liu, X., Zhao, H., Zhang, J., Zhang, J., Li, X., Zhang, Y., Bu, X., Shi, M., et al. (2014). Discoidin domain receptor 2 (DDR2) promotes breast cancer cell metastasis and the mechanism implicates epithelial-mesenchymal transition programme under hypoxia. J. Pathol. *234*, 526–537.

Sander, E.A., and Barocas, V.H. (2009). Comparison of 2D fiber network orientation measurement methods. J. Biomed. Mater. Res. A *88*, 322–331.

Savagner, P. (2015). Epithelial-mesenchymal transitions: from cell plasticity to concept elasticity. Curr. Top. Dev. Biol. *112*, 273–300.

Schedin, P., and Keely, P.J. (2011). Mammary gland ECM remodeling, stiffness, and mechanosignaling in normal development and tumor progression. Cold Spring Harb. Perspect. Biol. *3*, a003228.

Seguin, L., Desgrosellier, J.S., Weis, S.M., and Cheresh, D.A. (2015). Integrins and cancer: regulators of cancer stemness, metastasis, and drug resistance. Trends Cell Biol. *25*, 234–240.

Sivakumar, L., and Agarwal, G. (2010). The influence of discoidin domain receptor 2 on the persistence length of collagen type I fibers. Biomaterials *31*, 4802–4808.

Toy, K.A., Valiathan, R.R., Núñez, F., Kidwell, K.M., Gonzalez, M.E., Fridman, R., and Kleer, C.G. (2015). Tyrosine kinase discoidin domain receptors DDR1 and DDR2 are coordinately deregulated in triple-negative breast cancer. Breast Cancer Res. Treat. *150*, 9–18.

Tran, H.D., Luitel, K., Kim, M., Zhang, K., Longmore, G.D., and Tran, D.D. (2014). Transient SNAIL1 expression is necessary for metastatic competence in breast cancer. Cancer Res. *74*, 6330–6340.

Van Keymeulen, A., Rocha, A.S., Ousset, M., Beck, B., Bouvencourt, G., Rock, J., Sharma, N., Dekoninck, S., and Blanpain, C. (2011). Distinct stem cells contribute to mammary gland development and maintenance. Nature *479*, 189–193.

Vargo-Gogola, T., and Rosen, J.M. (2007). Modelling breast cancer: one size does not fit all. Nat. Rev. Cancer *7*, 659–672.

Wagner, K.U., McAllister, K., Ward, T., Davis, B., Wiseman, R., and Hennighausen, L. (2001). Spatial and temporal expression of the Cre gene under the control of the MMTV-LTR in different lines of transgenic mice. Transgenic Res. *10*, 545–553.

Walker, R.A. (2001). The complexities of breast cancer desmoplasia. Breast Cancer Res. *3*, 143–145.

Xu, H., Bihan, D., Chang, F., Huang, P.H., Farndale, R.W., and Leitinger, B. (2012). Discoidin domain receptors promote $\alpha1\beta1$- and $\alpha2\beta1$-integrin mediated cell adhesion to collagen by enhancing integrin activation. PLoS ONE *7*, e52209.

Yang, J., Wheeler, S.E., Velikoff, M., Kleaveland, K.R., LaFemina, M.J., Frank, J.A., Chapman, H.A., Christensen, P.J., and Kim, K.K. (2013). Activated alveolar epithelial cells initiate fibrosis through secretion of mesenchymal proteins. Am. J. Pathol. *183*, 1559–1570.

Zhang, K., Corsa, C.A., Ponik, S.M., Prior, J.L., Piwnica-Worms, D., Eliceiri, K.W., Keely, P.J., and Longmore, G.D. (2013). The collagen receptor discoidin domain receptor 2 stabilizes SNAIL1 to facilitate breast cancer metastasis. Nat. Cell Biol. *15*, 677–687.

Zhang, S., Bu, X., Zhao, H., Yu, J., Wang, Y., Li, D., Zhu, C., Zhu, T., Ren, T., Liu, X., et al. (2014). A host deficiency of discoidin domain receptor 2 (DDR2) inhibits both tumour angiogenesis and metastasis. J. Pathol. *232*, 436–448.